



ОБЪЕДИНЕННЫЙ
ИНСТИТУТ
ЯДЕРНЫХ
ИССЛЕДОВАНИЙ

Дубна

99-313

E2-99-313 e

M.V.Tokarev¹, O.V.Rogachevski², T.G.Dedovich³

SCALING FEATURES OF π^0 -MESON PRODUCTION
IN HIGH-ENERGY pp -COLLISIONS

Submitted to «Journal of Physics G: Nuclear and Particle Physics»

¹E-mail: tokarev@sunhe.jinr.ru

²E-mail: rogach@sunhe.jinr.ru

³E-mail: dedovich@sunhe.jinr.ru

1 Introduction

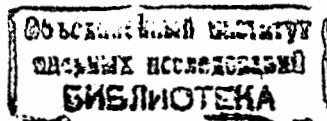
High transverse hadron production in pp collisions provides basic information on fundamental properties of colliding objects, their constituents and interaction itself. Perturbative QCD (pQCD) is widely used to explain and describe hadron spectra in pp [1] and their modification in pA and AA collisions [2, 3]. Although a high colliding energy and transverse momentum are necessary conditions to use pQCD nevertheless parton fragmentation into hadrons might be one of the least understandable features of QCD [4] up to now. Even though a primary scattering process is described in terms of pQCD, the hadronization chain contains very low p_{\perp} hadrons with respect to the parent parton. Therefore, the whole process is clearly a nonperturbative phenomenon involving final state interactions which have to conserve color and baryon numbers.

A comparison of high p_{\perp} hadrons produced in hadron-hadron, hadron-nucleus and nucleus-nucleus interactions both in the central and non-central rapidity region allows us to understand in detail the physics phenomena underlying secondary hadron production and, in particular, the hadronization process in nuclear matter.

In this paper, we develop the method proposed in [5, 6] for the description of π^0 -meson production in pp collisions at high energies. In the framework of the method, such experimental observables as inclusive cross section and multiplicity charged particle density are used to construct the scaling function $\psi(z)$ and variable z . The scaling, known as z -scaling, reveals interesting properties. Two of them are the energy and angular independence of the scaling function, $\psi(z)$, of produced objects (hadrons [6, 7], photons [8, 9, 10], and jets [11]). The properties of the scaling are assumed to reflect the fundamental properties of particle structure, interaction and production. According to [5, 6] the physics meaning of the scaling function $\psi(z)$ is the probability to form the produced particle with formation length z . The existence of the scaling itself means that the hadronization mechanism of particle production reveals such fundamental properties as self-similarity, locality, fractality and scale-relativity [12].

The scaling properties of inclusive π^0 -meson production in pp collisions at high energies are studied in this paper. The available experimental data on the cross section obtained at ISR are used to construct the scaling function $\psi(z)$. The properties of data z -presentation are verified. The $\psi(z)$ dependence on the energy \sqrt{s} and angles θ of produced π^0 -mesons is studied. A new feature of data z -presentation for π^0 -meson production, power behaviour of the scaling function $\psi(z) \simeq z^{-\alpha}$, is found. The properties of z -scaling for π^0 -mesons produced in pp collisions are used to predict meson yields at RHIC and LHC energies.

The paper is organized as follows. A general concept of z -scaling and the method of constructing the scaling function for hadron production in pp collisions are shortly described in Section 2. New results on the energy and angular independence of scaling function for π^0 -meson production in pp collisions based on the analysis of the experimental data, discussion of the obtained results, physical interpretation of the scaling function and variable z are presented in Section 3. Conclusions are summarized in Section 4.



2 Z-scaling

In this section, we would like to remember basic ideas of z-scaling [5, 6] dealing with the investigation of the inclusive process

$$P_1 + P_2 \rightarrow q + X. \quad (1)$$

The momenta and masses of colliding nuclei and inclusive particle are denoted by P_1, P_2, q and M_1, M_2, m_1 , respectively. In accordance with Stavinsky's ideas [13], the gross features of the inclusive particle distributions for reaction (1) at high energies can be described in terms of the corresponding kinematic characteristics of the exclusive subprocess written in the symbolic form

$$(x_1 M_1) + (x_2 M_2) \rightarrow m_1 + (x_1 M_1 + x_2 M_2 + m_2). \quad (2)$$

The parameter m_2 is introduced to satisfy internal conservation laws (for isospin, baryon number, and strangeness). The x_1 and x_2 are the scale-invariant fractions of the incoming four-momenta P_1 and P_2 of colliding objects. The energy of the parton subprocess defined as

$$\hat{s}_z^{1/2} = \sqrt{(x_1 P_1 + x_2 P_2)^2} \quad (3)$$

represents the center-of-mass energy of the constituents involved in the collision. In accordance with a space-time picture of hadron interactions at the parton level, the cross section for the production of the inclusive particle is governed by a minimum energy of colliding partons

$$d\hat{\sigma}/dt \sim 1/\hat{s}_{min}^2(x_1, x_2). \quad (4)$$

The corresponding energy $\hat{s}_{min}^{1/2}$ is fixed as a minimum of Eq. (3) which is necessary for the production of the secondary particle with mass m_1 and four-momentum q . Below we present a scheme from which a more general structure of the variables x_1 and x_2 follows.

We would like to emphasize two main points of this approach. The first one is a fractal character of the parton content of the involved composite structures. The second one is self-similarity of the mechanism underlying particle production at the level of elementary constituent interactions. Both points will be discussed in the other sections.

2.1 Fractions x_1 and x_2

The elementary parton-parton collision is considered as a binary subprocess which is satisfied the condition

$$(x_1 P_1 + x_2 P_2 - q)^2 = (x_1 M_1 + x_2 M_2 + m_2)^2. \quad (5)$$

The equation expresses the 4-momentum conservation law for binary parton-parton collisions in which the inclusive particle with momentum q can be produced.

Relationship between x_1 and x_2 is written in the form

$$x_1 x_2 - x_1 \lambda_2 - x_2 \lambda_1 = \lambda_0, \quad (6)$$

where $\lambda_i = \lambda_i(P_1, P_2, q, M_1, M_2, m_2)$ are the known functions of particle momenta and masses [6]. Considering process (2) as a parton-parton collision, we introduce the coefficient Ω which connects kinematic and dynamic characteristics of the interaction. The coefficient is chosen in the form

$$\Omega(x_1, x_2) = m(1-x_1)^{\delta_1}(1-x_2)^{\delta_2}, \quad (7)$$

where m is the mass constant and δ_1 and δ_2 are the factors relating the fractal structure of colliding objects [6]. We define the fractions x_1 and x_2 to maximize the value of $\Omega(x_1, x_2)$, simultaneously fulfilling condition (6)

$$d\Omega(x_1, x_2)/dx_1 = 0. \quad (8)$$

A prominent expression for $x_{1,2} = x_{1,2}(\lambda_0, \lambda_1, \lambda_2, \delta_1, \delta_2)$ was obtained in [6]. A physical interpretation of the coefficient Ω and factors δ_2 and δ_1 of is given in Sec. IV.

Equation (6) satisfies the 4-momentum conservation law in the whole phase space. The variables $x_{1,2}$ are equal to unity along the phase space boundary and cover the full phase space accessible at any energy. The restriction $\lambda_1 + \lambda_2 + \lambda_0 \leq 1$ can be obtained from the condition $x_i \leq 1$. The inequality corresponds to the threshold condition

$$(M_1 + M_2 + m_2)^2 + E^2 - m_1^2 \leq (\sqrt{s} - E)^2. \quad (9)$$

Here, \sqrt{s} and E are the energy in the reaction center-of-mass and the energy of the produced inclusive particle, respectively. Inequality (9) bounds kinematically a maximum energy E of the inclusive particle m_1 in the c.m.s. of reaction (1).

2.2 Definition of scaling function $\psi(z)$ and variable z

In accordance with the self-similarity principle, we search for the solution depending on a single scaling variable z in the form

$$\psi(z) \equiv \frac{1}{\langle N \rangle \sigma_{inel}} \frac{d\sigma}{dz}. \quad (10)$$

Here, σ_{inel} is the inelastic cross section and $\langle N \rangle$ is the average charged particle multiplicity. The function $\psi(z)$ is chosen to be only dependent on the scaling variable z . All the quantities refer to pp interactions. The function ψ expressed via the invariant differential cross section for the production of the inclusive particle m_1 and is introduced as follows (see Ref.[6])

$$\psi(z) = \frac{\pi s}{\rho \sigma_{inel}} J^{-1} E \frac{d\sigma}{dq^3}, \quad (11)$$

where the factor J is given by $J = |\partial y / \partial \lambda_1 \cdot \partial z / \partial \lambda_2 - \partial y / \partial \lambda_2 \cdot \partial z / \partial \lambda_1|$. Here, s is the center-of-mass energy squared of the corresponding NN -system. Expression (11) relates the inclusive differential cross section and the average multiplicity density $\rho(s, \eta) = d \langle N \rangle / d\eta$ to the scaling function $\psi(z)$. The combination $y = 0.5 \ln(\lambda_2 / \lambda_1)$ is approximated to (pseudo)rapidity η at high energies.

We choose z as a physically meaningful variable which could reflect self-similarity (scale invariance) as a general pattern of hadron production in accordance with the

ansatz suggested in [6]

$$z = \frac{\sqrt{\hat{s}_\perp}}{\Omega \cdot \rho(s)}, \quad (12)$$

where $\hat{s}_\perp^{1/2}$ is the transverse kinetic energy of subprocess (2), defined by the expression $\hat{s}_\perp^{1/2} = \hat{s}_\lambda^{1/2} + \hat{s}_x^{1/2} - m_1 - (M_1 x_1 + M_2 x_2 + m_2)$; Ω is the fractal measure given by (7) and $\rho(s) = dN/d\eta|_{\eta=0}$ is the average multiplicity density of charged particles produced in the central rapidity region of the corresponding nucleon-nucleon interaction.

The transverse energy consists of two parts

$$\hat{s}_\lambda^{1/2} = \sqrt{(\lambda_1 P_1 + \lambda_2 P_2)^2}, \quad \hat{s}_x^{1/2} = \sqrt{(\chi_1 P_1 + \chi_2 P_2)^2}, \quad (13)$$

which represent the transverse energy of the inclusive particle and its recoil, respectively. We would like to note that the form of z , as defined by Eqs. (12) and (7), determines its variation range. The boundaries of the range are 0 and ∞ . These values are scale independent and kinematically accessible at any energy.

2.3 Fractality and scale-relativity

Here, we discuss such a property of z -scaling construction as fractality. Fractality as a general principle in particle and nuclear physics means that the internal structure of particles and their interactions reveal self-similarity on any scale.

Equation (6) describes the 4-momentum conservation law for an elementary subprocess. The equation is a covariant one under the scale transformation

$$\lambda_{1,2} \rightarrow \rho_{1,2} \cdot \lambda_{1,2}, \quad x_{1,2} \rightarrow \rho_{1,2} \cdot x_{1,2}, \quad \lambda_0 \rightarrow \rho_1 \cdot \rho_2 \cdot \lambda_0. \quad (14)$$

The transformation with the scale parameters $\rho_{1,2}$ allows us to consider the collision of complex objects in terms of a suitable subprocess of interacting elementary constituents. The choice of the elementary subprocess suitable to the problem is important to develop a microscopic scenario of the collision and, in particular, to estimate a relative contribution of rescattering and multiscattering mechanisms.

The coefficient Ω connects the kinematic and dynamic characteristics of the interaction. The factors δ_1 and δ_2 are related to the fractal structure of colliding objects. The fractal structure itself is defined by the structure of interacting constituents which is not an elementary one either. In this scheme, hadron-hadron, hadron-nucleus and nucleus-nucleus collisions are considered as an interaction of two fractals. The measure of the interaction is written as

$$\Omega = V^\delta(x_1, x_2) \quad (15)$$

where δ is the coefficient (fractal dimension) describing the fractal structure of the elementary collision. The factor V is part of the full phase-space of fractions $\{x_1, x_2\}$ corresponding to that sort of parton-parton collisions in which the inclusive particle can be produced. The fractal property of a collision reveals itself so that only the part of all multiscatterings corresponding to the phase space V^δ produces the

* The fractions χ_i are the known functions of λ_i [6].

inclusive particle. The measure Ω is an invariant under simultaneity of the scale transformation of Lorenz invariants x_i and multiplicative transformation of δ_i . It describes a correlation between the fraction x_i and the fractal dimension δ . Therefore, the relativity principle could be applied, besides the laws of motion, to the laws of scale [12], as well. In the considered perspective, the principle of scale relativity states that the Einstein-Lorenz composition law of velocities is applicable to the systems of reference whatever their state of scale [12].

3 π^0 -meson production and z -scaling

In this section, we study the properties of z -scaling for π^0 -mesons produced in pp collisions. General formulas (11) and (12) are used to calculate the scaling function $\psi(z)$ and the variable z . The quantities $\rho(s, \eta)$ and σ_{inel} are the average charged particle multiplicity density and the inelastic cross section of pp -collisions, respectively.

3.1 Energy independence of $\psi(z)$

Let us now study the energy dependence of the scaling function $\psi(z)$ of π^0 production in pp collisions. For analysis, we use the sets of cross section data [14]-[25] obtained at ISR. It should be noted that a strong dependence of the cross section on energy \sqrt{s} was experimentally found. The effect increases with transverse momentum.

We verify the hypothesis of energy scaling for data z -presentation for π^0 -meson production in pp collisions using the available experimental data.

Figures 1(a)-7(a) show the dependence of the cross section of the $p + p \rightarrow \pi^0 + X$ process on transverse momentum q_\perp at $\sqrt{s} = 23, 30, 45, 53$ and 63 GeV [14]-[25] and a produced angle of 90° . We would like to note that the data cover a wide transverse momentum range, $q_\perp = 1 - 14$ GeV/c.

Some features of π^0 -meson spectra should be noted. The first one is a strong energy dependence of the cross section on transverse momentum. The second feature is a tendency to increase the difference between π^0 -meson yield with transverse momentum and energy \sqrt{s} . The third one is a nonexponential behaviour of the spectra at $q_\perp > 4$ GeV/c.

Figures 1(b)-7(b) show z -presentation of the same data sets. Taking the experimental errors, into account, we can conclude that the scaling function $\psi(z)$ of π^0 -meson production in pp collisions demonstrates an energy independence over a wide energy and transverse momentum range at $\theta = 90^\circ$.

3.2 Angular independence of $\psi(z)$

To analyze the angular dependence of the scaling function $\psi(z)$ of π^0 -meson production in pp collisions, we use the data sets obtained at ISR [18, 20]. The first set includes the results of measurements of the invariant cross section $Ed^3\sigma/dq^3$

at colliding energies $\sqrt{s} = 23$ and 53 GeV over momentum and angular ranges of $q_{\perp} = 1.5 - 4.25$ GeV/c and $\theta = 5^{\circ} - 90^{\circ}$, respectively. The second one was obtained at $\sqrt{s} = 63$ GeV. The produced π^0 -mesons were registered over transverse momentum ranges of $q_{\perp} = 1.05 - 4.3$ GeV/c and a rapidity interval of $\eta = 2 - 2.75$. A strong dependence of the cross section on the angle of the produced π^0 -meson was experimentally found. Here, we describe the procedure of data z -analysis [18, 20].

We verify the hypothesis of angular scaling for data z -presentation for π^0 -meson spectra.

Figure 8(a) shows the dependence of the cross section of the $p + p \rightarrow \pi^0 + X$ process on transverse momentum q_{\perp} at $\sqrt{s} = 63$ [19] for different rapidity intervals, $\eta = 2 - 2.25, 2.25 - 2.5$ and $2.5 - 2.75$.

Figures 9(a) and 10(a) present the spectra as a function of q_{\perp} at $\sqrt{s} = 23$ GeV and 53 GeV over a wide angular range of $\theta = 5^{\circ} - 90^{\circ}$.

Figures 8(b)-10(b) demonstrate z -presentation of the same data sets. The obtained results show that the function $\psi(z)$ is independent of angle θ over a wide range at ISR energies.

3.3 Power law of $\psi(z)$ and fractality

Here, we discuss a new feature of data z -presentation for π^0 -meson production. This is the power law of the scaling function, $\psi(z) \sim z^{-\alpha}$.

From Figures 1(b) and 7(b) one can see that the data sets demonstrate a linear z -dependence of $\psi(z)$ on the log-log scale at $q_{\perp} > 4$ GeV/c. The results of our analysis of the coefficient α are presented in Table 1. The parameter α is the slope parameter of z -dependence of $\psi(z)$ on the log-log scale.

Table 1. Fractal dimension α of the scaling function, $\psi(z) \sim z^{-\alpha}$, of π^0 -mesons produced in pp collisions at a high transverse momentum

| \sqrt{s} , GeV | α | Ref. |
|------------------|----------|------|
| 30 | 7.47 | [14] |
| 53 | 7.45 | [14] |
| 63 | 7.10 | [14] |
| 63 | 7.43 | [20] |
| 53 | 6.82 | [24] |
| 63 | 7.65 | [24] |
| 53 | 7.19 | [25] |

The mean value $\bar{\alpha}$ and dispersion σ calculated using the formulas

$$\bar{\alpha} = \frac{1}{n} \sum_i \alpha_i, \quad \sigma^2 = \frac{1}{n-1} \sum_i (\alpha_i - \bar{\alpha})^2 \quad (16)$$

were found to be $\bar{\alpha} = 7.30$ and $\sigma = 0.28$, respectively.

Figure 11 shows q_{\perp} - and z -presentation of the cross section data [14, 15, 17, 18, 21]. Taking into account the accuracy of the available experimental data, we can conclude that the behaviour of $\psi(z)$ for π^0 -mesons produced in pp collisions reveals

a power dependence and the value of the slope parameter α_{pp} is independent of colliding energy \sqrt{s} over a wide range of high transverse momentum q_{\perp} .

For comparison with the pp case (see Figure 11), Figure 12 demonstrates the dependence of the cross section $E d^3\sigma/dq^3$ on q_{\perp} and the scaling function $\psi(z)$ on z for the $\bar{p} + p \rightarrow \pi^0 + X$ process at $\sqrt{s} = 540$ GeV. The data were obtained by the UA2 collaboration at SpS [26]. The produced π^0 -mesons were registered over a transverse momentum range of $q_{\perp} = 0.29 - 41$ GeV/c and a rapidity of $\eta = 0$ and 1.4. The power behaviour of the function $\psi(z)$ on the log-log scale at $q_{\perp} > 4$ GeV/c was observed and, the slope parameter $\alpha_{\bar{p}p}$ was found to be 5.75 ± 0.04 .

The values of the slope parameter for π^0 -meson production in pp and $\bar{p}p$ collisions were found to be different ones so that $\alpha_{pp} > \alpha_{\bar{p}p}$.

We would like to emphasize that the power behaviour is a new feature of the scaling function found for π^0 -meson production at high q_{\perp} *. From our point of view, the existence of the power law, $\psi(z) \sim z^{-\alpha}$, means that π^0 -meson formation reveals a fractal behaviour.

3.4 Multiplicity density of charged particles

The average multiplicity density, $\rho(s, \eta)$, of charged particles is an important element for z -scaling construction. Both scaling function (11) and variable z (12) are expressed via $\rho(s, \eta)$.

Figure 14 shows the average multiplicity density $\rho(s)$ of charged particles produced in pp and $\bar{p}p$ collisions in the central rapidity range as a function of NN center-of-mass energy \sqrt{s} . The experimental data are taken from [27]-[31]. The fit to the inelastic data in the form $\rho(s) = 0.74s^{0.105}$ [28, 29] is shown by a dashed line. The other points corresponds to nonsingle diffractive events. The bars shown in Figure 14 at $\sqrt{s} = 100$ GeV correspond to 10% errors. It should be emphasized that high accuracy measurements of absolute cross section normalization and the multiplicity density of charged particles are very important to verify the energy independence of the scaling function.

4 Discussion

Based on the available experimental data of π^0 -meson production in pp collisions, we have established that the scaling function $\psi(z)$ is energy and angular independent over a wide range of \sqrt{s} and θ . Moreover, the z -dependence of $\psi(z)$ reveals a new property, a power behaviour $\psi(z) \sim z^{-\alpha}$, over a high transverse momentum range ($q_{\perp} > 4$ GeV/c). We would like to emphasize that z -scaling was observed in production of particles with high q_{\perp} at high energies. This means that the scaling function describes the fragmentation process of point-like produced partons into observable hadrons.

In this section, we qualitatively discuss the obtained results in the framework of a fractal picture of constituent interaction. The idea of fractality of constituents

* The power law of the scaling function was found for direct photon and jet production in $\bar{p}p$ and pp collisions [8, 9].

(hadrons, nuclei etc.) and their interactions is its substantial element. Fractality as a general principle in particle physics means that the internal structure of particles and their interactions reveal self-similarity on any scale mathematically described by the power law.

The fractal character of initial states regarding the parton compositeness of hadrons reveals itself with a larger resolution at high energies and a high transverse momentum. Led by these principles, the variable z is constructed according to Eq.(12). The fractal objects are usually characterized by a power law dependence of their fractal measures [12]. The fractal measure, considered in our case, is given by all possible configurations of elementary interactions that lead to the production of a hadron.

The fractal measure $\Omega(x_1, x_2)$ taken in the form

$$\Omega(x_1, x_2) \sim [(1-x_1)(1-x_2)]^\delta$$

is described by the power law in the space of fractions $\{x_1, x_2\}$. The measure reflects the number of constituent configurations in the colliding objects involved in hadron production. The measure is characterized by the fractal dimension δ [6]. In the framework of a fractal picture, the number of initial configurations is maximized according to Eq.(8), and the variable z describes the energy of an elementary constituent collision per initial configuration and per produced particle.

The existence of z -scaling itself is the confirmation of hadron interaction self-similarity at the constituent level. At the same time the existence of the power law at the constituent level is the confirmation of the fractal structure of constituents themselves.

As one can see from Figure 11(b), the violation of the power behaviour is observed at $q_\perp < 4 \text{ GeV}/c$. According to the general idea that the function $\psi(z)$ describes the hadronization mechanism, we interpret a different behaviour of the function as a transition from the soft to hard regime of hadron formation. In contrast to the soft one the hard regime corresponds to fractal hadronization (the power law of $\psi(z)$).

Here, we suggest a scenario of hadron formation. The hadronization process in which the produced bare quark dresses itself dragging out some matter of the vacuum forming the dressed quark is a self-similar one. It is reasonable to assume that hadron formation depends on the transverse momentum characterizing the compositeness of colliding objects. The faster dressing the smaller p_\perp . We interpret the power behaviour of ψ at a high transverse momentum as an indication that the quantity of matter dragged out during the particle formation is limited. The saturation of absorption energy by "dressing" quark takes place.

The results presented in Figure 11(b) give direct evidence of the asymptotic regime of π^0 -meson formation with increasing transverse momentum. The slope parameter α is independent of \sqrt{s} and q_\perp over a relatively wide kinematic range. A similar asymptotic behaviour of $\psi(z)$ was found for η^0 -meson production in pp collisions, too. Figure 13 shows q_\perp - and z -presentation of the experimental cross section data [32].

In the framework of the proposed scenario, the mechanism of hadron formation is considered as a dynamic process of construction of a complex fractal (hadron, jet etc.) from elementary fractal blocks (interacting constituents). The size and

structure of the blocks depend on the colliding energy and transverse momentum of the produced object. The value of z is proportional to the number of steps needed to construct a complex object (fractal) from the elementary blocks. It can be considered as a relative formation length. From our point of view, this power law reflects the fractality of hadron formation itself.

We assume that inhomogeneous domains (for example, DCC [33]), a new type of interaction, quark compositeness and features of hadronization in the transition phase of nuclear matter may be responsible for the z -scaling violation. The change of fractal dimension α of the hadron formation process is a quantitative characteristic of such violation.

We use the properties of the scaling function $\psi(z)$ for pp and $\bar{p}p$ collisions to predict π^0 - and η^0 -meson spectra at RHIC and Tevatron energies.

Figure 15(a) shows the $Ed^3\sigma/dq^3$ dependence on transverse momentum of π^0 -mesons produced in pp collisions in the central rapidity range at a different colliding energy. The points (\star, \diamond) and solid lines are the calculated results at $\sqrt{s} = 200$ and 500 GeV . The experimental data, $\triangle - 30 \text{ GeV}$, $\circ - 53 \text{ GeV}$, $+ - 62 \text{ GeV}$, are taken from [14].

Figure 15(b) presents π^0 -meson yields in $\bar{p}p$ collisions at $\sqrt{s} = 63, 540$ and 2000 GeV . The experimental data, $+ - 540 \text{ GeV}$, are taken from [26].

The spectra of η^0 -mesons produced in pp collisions as a function of transverse momentum q_\perp at $\sqrt{s} = 30 - 500 \text{ GeV}$ are shown in Figure 15(c).

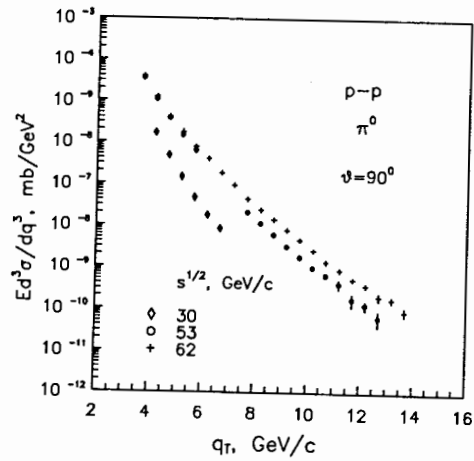
5 Conclusions

The inclusive π^0 -meson production in pp collisions at high energies is considered in the framework of a general concept of z -scaling. The function $\psi(z)$ describing the new scaling of π^0 -meson production is constructed and used to verify the energy and angular independence. The experimental data on the inclusive cross sections over a high transverse momentum range, colliding energy and rapidity range obtained at ISR are used for the analysis.

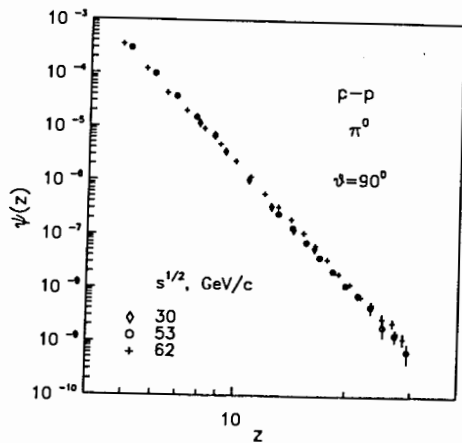
The function $\psi(z)$, representing a new presentation of experimental data, is expressed via the invariant inclusive cross section $Ed^3\sigma/dq^3$ and normalized to the multiplicity density of charged particles produced in pp collisions.

The energy and angular independence of the scaling function $\psi(z)$ is found. The function $\psi(z)$ is interpreted as the quantity being proportional to the probability to form a hadron with formation length z . The scaling function $\psi(z)$ of π^0 -meson production demonstrates the power behaviour, $\psi(z) \sim z^{-\alpha}$ over a high transverse momentum range of $q_\perp > 4 \text{ GeV}/c$. The mean values of the slope parameter (the fractal dimension of hadron formation), α , for π^0 -meson production in pp and $\bar{p}p$ interactions are found to be 7.30 ± 0.28 and 5.75 ± 0.04 , respectively. The value of the slope parameter α_{pp} is independent of colliding energy \sqrt{s} and transverse momentum q_\perp .

A new presentation of the experimental cross section data of η^0 -mesons produced in pp collisions is found to have similar features. The slope parameter α_{pp}^η for the process is found to be 7.70 ± 0.06 .

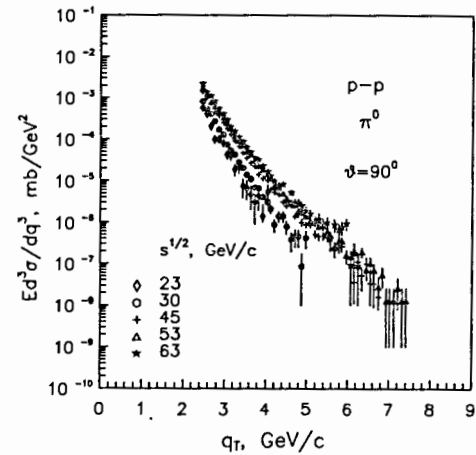


a)

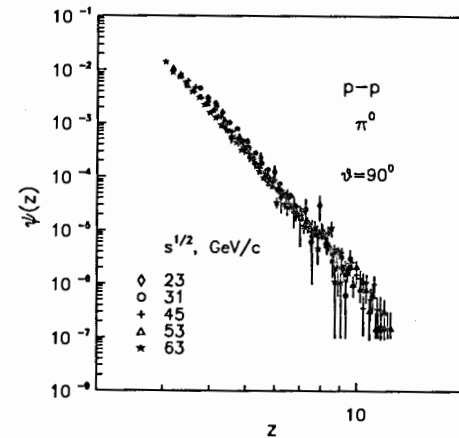


b)

Figure 1. (a) The dependence of the inclusive cross section of π^0 -meson production on transverse momentum q_{\perp} in pp collisions at $\sqrt{s} = 30, 53$ and 62 GeV and an angle θ of 90° . The experimental data on the cross section are taken from [14]. (b) The corresponding scaling function $\psi(z)$.



a)



b)

Figure 2. (a) The dependence of the inclusive cross section of π^0 -meson production on transverse momentum q_{\perp} in pp collisions at $\sqrt{s} = 23, 30, 45, 53$ and 63 GeV and an angle θ of 90° . The experimental data on the cross section are taken from [22]. (b) The corresponding scaling function $\psi(z)$.

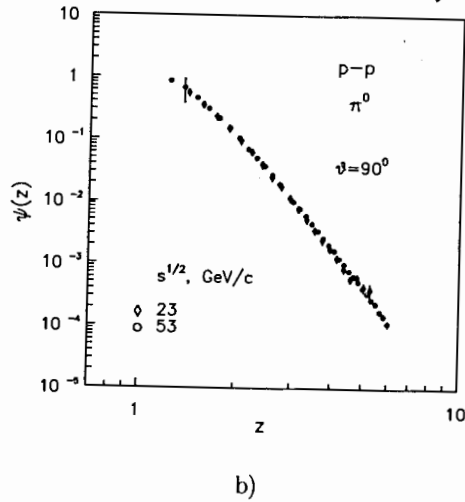
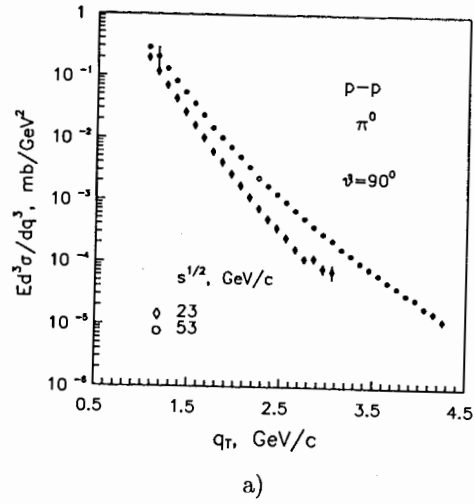


Figure 3. (a) The dependence of the inclusive cross section of π^0 -meson production on transverse momentum q_{\perp} in pp collisions at $\sqrt{s} = 23$ and 53 GeV and an angle θ of 90° . The experimental data on the cross section are taken from [18]. (b) The corresponding scaling function $\psi(z)$.

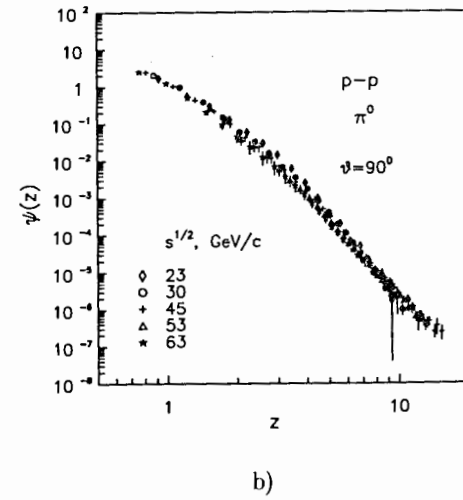
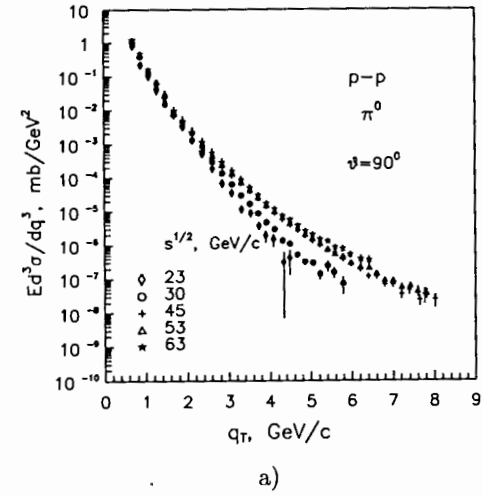
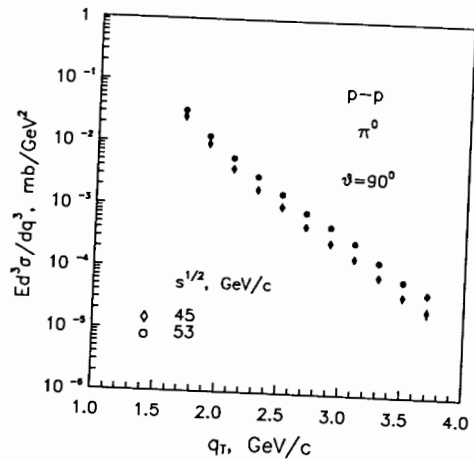
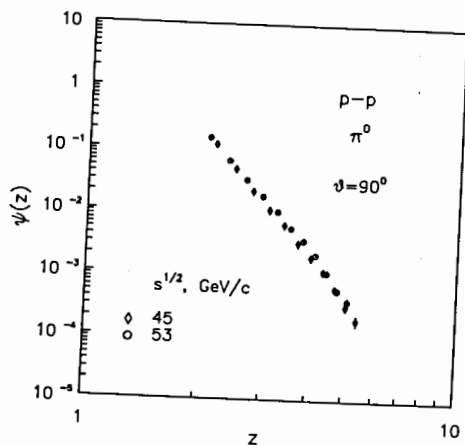


Figure 4. (a) The dependence of the inclusive cross section of π^0 -meson production on transverse momentum q_{\perp} in pp collisions at $\sqrt{s} = 23, 30, 45, 53$ and 63 GeV and an angle θ of 90° . The experimental data on the cross section are taken from [21]. (b) The corresponding scaling function $\psi(z)$.

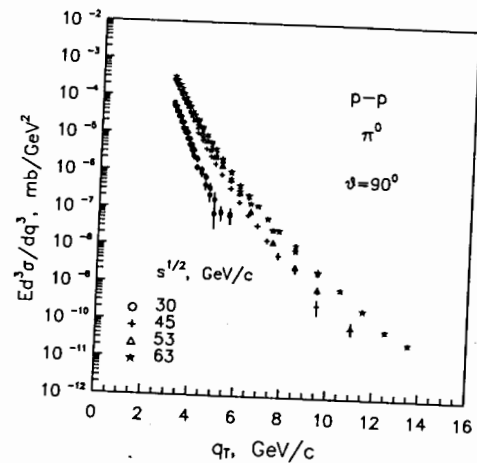


a)

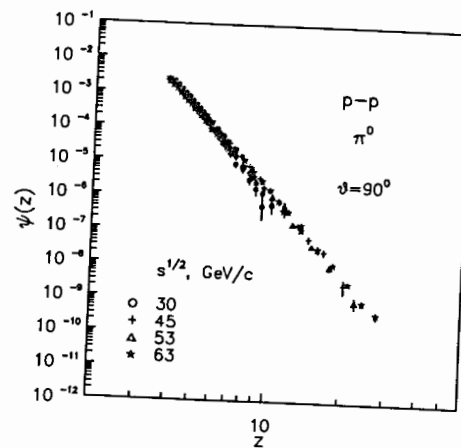


b)

Figure 5. (a) The dependence of the inclusive cross section of π^0 -meson production on transverse momentum q_{\perp} in pp collisions at $\sqrt{s} = 45$ and 63 GeV and an angle θ of 90° . The experimental data on the cross section are taken from [21]. (b) The corresponding scaling function $\psi(z)$.

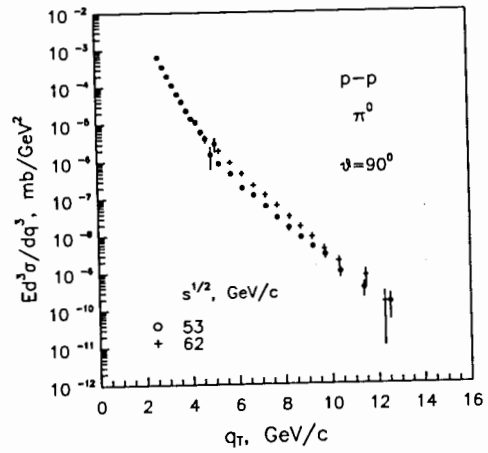


a)

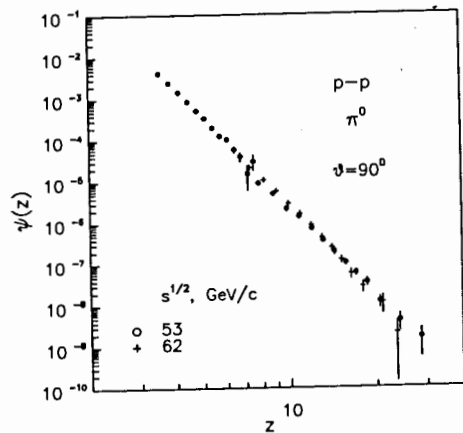


b)

Figure 6. (a) The dependence of the inclusive cross section of π^0 -meson production on transverse momentum q_{\perp} in pp collisions at $\sqrt{s} = 30, 45, 53$ GeV and 63 GeV and an angles θ of 90° . The experimental data on the cross section are taken from [15]-[17]. (b) The corresponding scaling function $\psi(z)$.

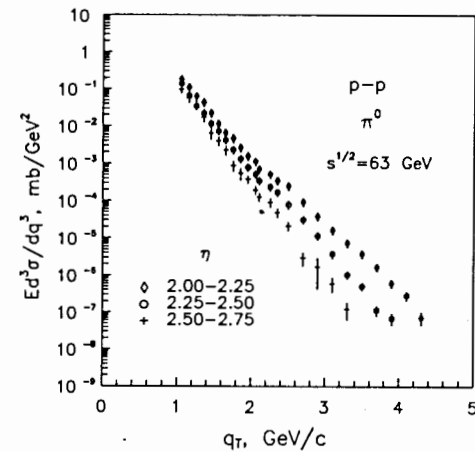


a)

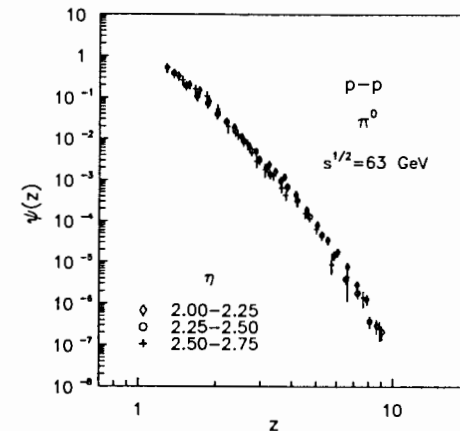


b)

Figure 7. (a) The dependence of the inclusive cross section of π^0 -meson production on transverse momentum q_{\perp} in pp collisions at $\sqrt{s} = 53$ and 62 GeV and an angle θ of 90° . The experimental data on the cross section are taken from [24, 25]. (b) The corresponding scaling function $\psi(z)$.



a)



b)

Figure 8. (a) The dependence of the inclusive cross section of π^0 -meson production on transverse momentum q_{\perp} in pp collisions at $\sqrt{s} = 63$ GeV and the rapidity $\eta = 2. - 2.75$. The experimental data on the cross section are taken from [19]. (b) The corresponding scaling function $\psi(z)$.

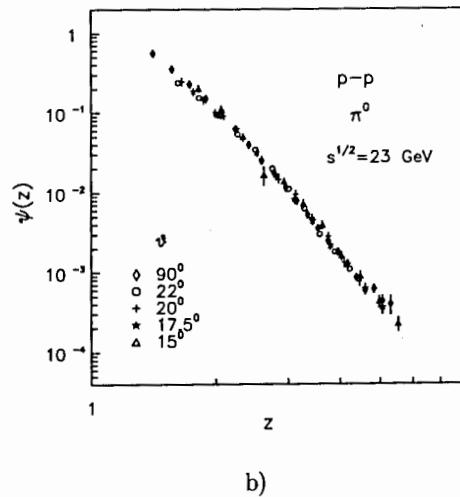
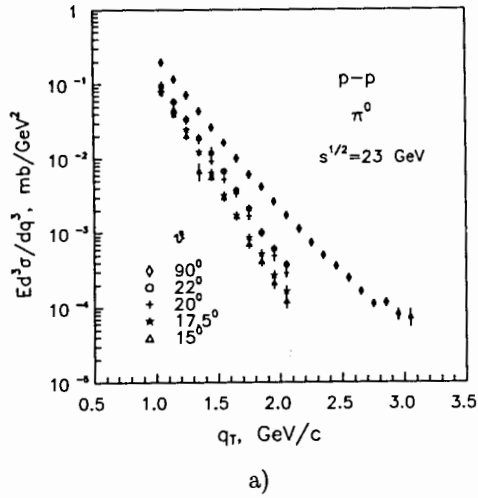


Figure 9. (a) The dependence of the inclusive cross section of π^0 -meson production in pp collisions at $\sqrt{s} = 23$ GeV and an angle θ on transverse momentum q_{\perp} . The experimental data on the cross section are taken from [18]. (b) The corresponding scaling function $\psi(z)$.

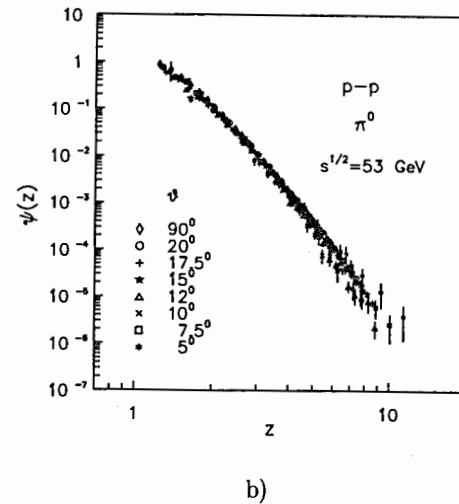
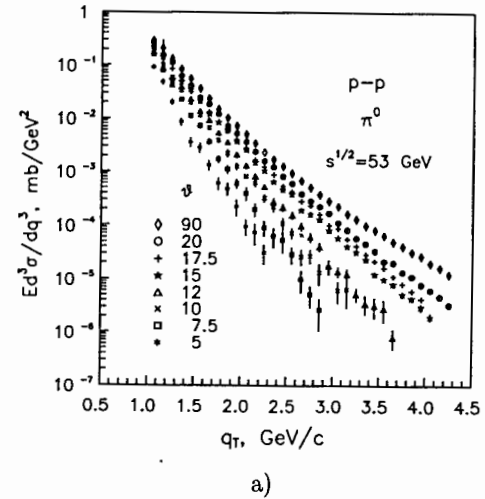
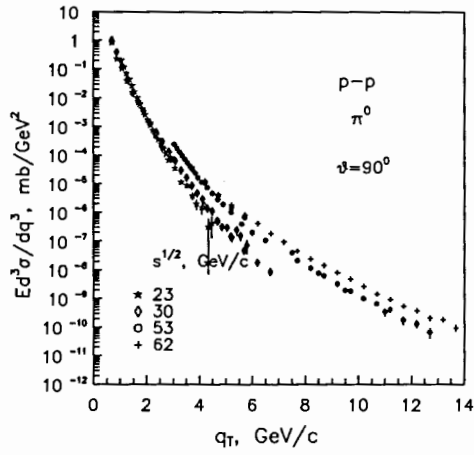
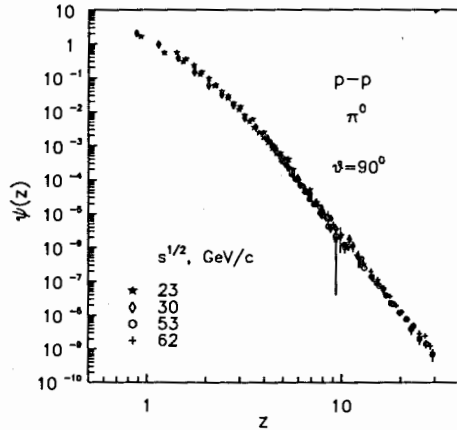


Figure 10. (a) The dependence of the inclusive cross section of π^0 -meson production in pp collisions at $\sqrt{s} = 53$ GeV and an angle θ on transverse momentum q_{\perp} . The experimental data on the cross section are taken from [18]. (b) The corresponding scaling function $\psi(z)$.

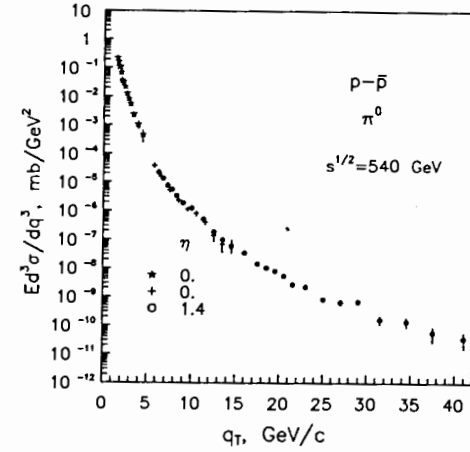


a)

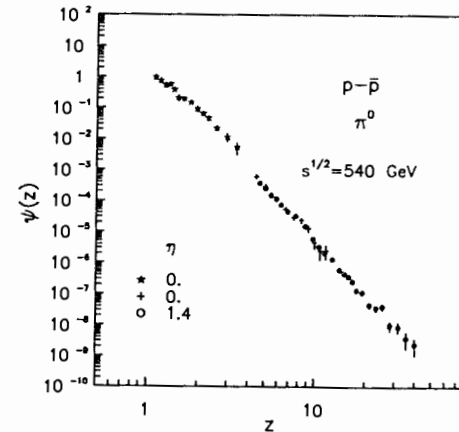


b)

Figure 11. (a) The dependence of the inclusive cross section of π^0 -meson production on transverse momentum q_{\perp} in pp collisions at $\sqrt{s} = 23, 30, 53$ and 62 GeV and an angle θ of 90° . The experimental data on the cross section are taken from [14, 15, 17, 18, 21]. (b) The corresponding scaling function $\psi(z)$.



a)



b)

Figure 12. (a) The dependence of the inclusive cross section of π^0 -meson production on transverse momentum q_{\perp} in $\bar{p}p$ collisions at $\sqrt{s} = 540$ GeV and a rapidity $\eta = 0, 1.4$. The experimental data on the cross section are taken from [26]. (b) The corresponding scaling function $\psi(z)$.

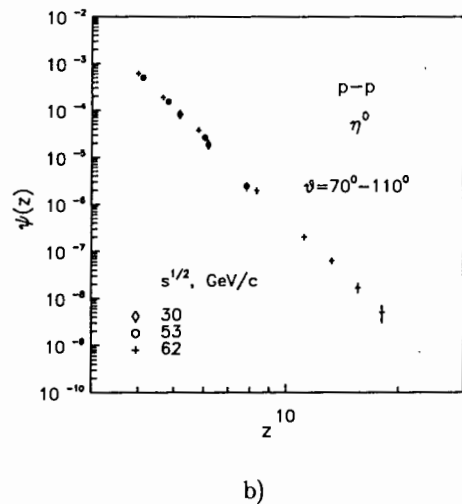
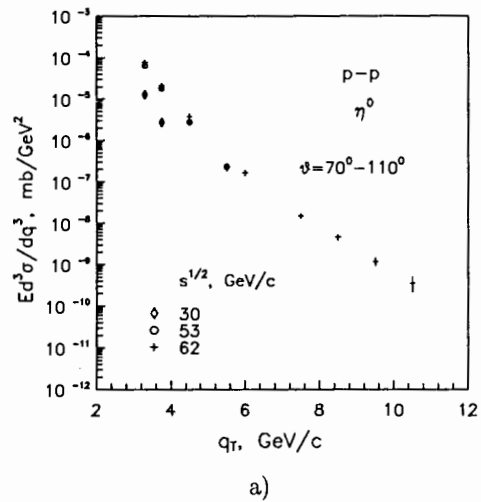


Figure 13. (a) The dependence of the inclusive cross section of η^0 -meson production on transverse momentum q_{\perp} in pp collisions at $\sqrt{s} = 30, 53$ and 62 GeV. The experimental data on the cross section are taken from [17]. (b) The corresponding scaling function $\psi(z)$.

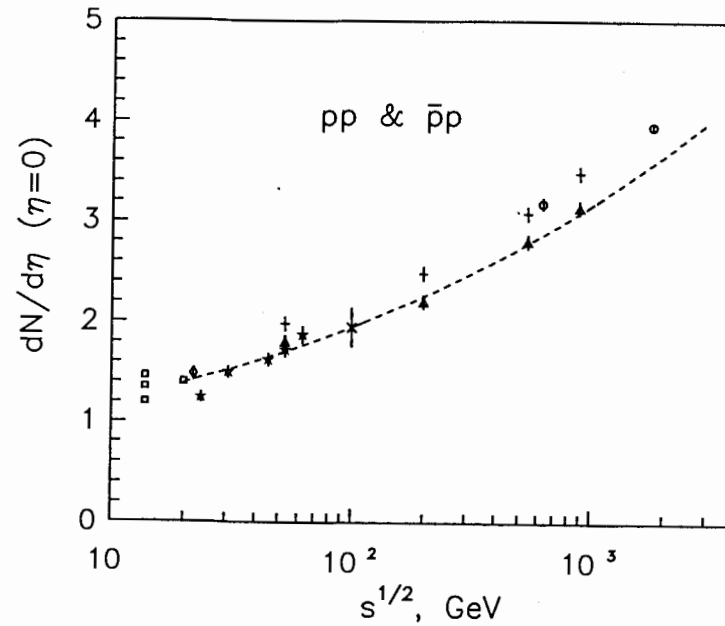
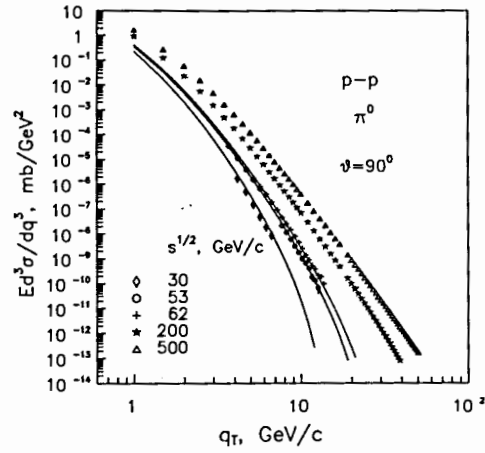
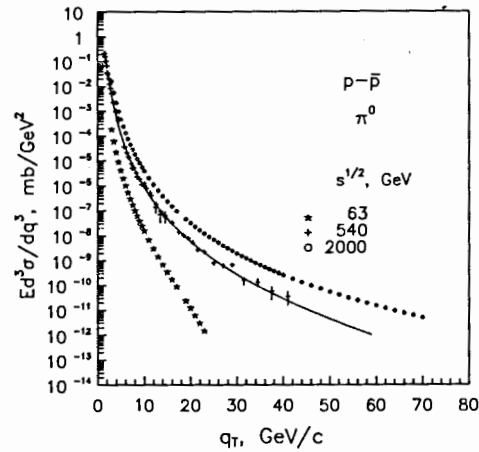


Figure 14. The multiplicity density of charged particles produced in pp and $\bar{p}p$ collisions as a function of \sqrt{s} at $\eta = 0$. The experimental data are taken from [27]-[31]. The fit to inelastic data is shown by a dashed line.



a)



b)

Figure 15. The dependence of the inclusive cross section of π^0 -meson production in pp and $p\bar{p}$ collisions on transverse momentum q_{\perp} . (a) The points (\star —200 GeV, Δ —500 GeV) and solid lines are the obtained results at different colliding energy \sqrt{s} . The experimental data, \diamond —30 GeV, \circ —53 GeV, \circ —62 GeV, are taken from [14]. (b) The points (\star —63 GeV, \circ —2000 GeV) and solid line are the results of our calculations. The experimental data, \circ —540 GeV, are taken from [26].

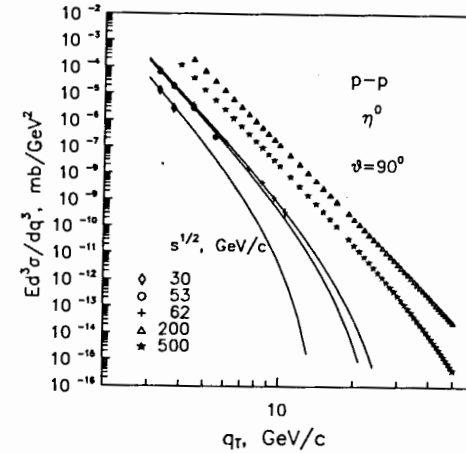


Figure 15 (c) The dependence of the inclusive cross section of η^0 -meson production in pp collisions on transverse momentum q_{\perp} . The points (\star —200 GeV, Δ —500 GeV) and solid lines are the results obtained at different colliding energy \sqrt{s} . The experimental data, \diamond —30 GeV, \circ —53 GeV, \circ —62 GeV, are taken from [32].

Using the scaling properties of $\psi(z)$, the dependence of the cross sections of π^0 - and η^0 -mesons produced in pp and $\bar{p}p$ collisions on transverse momentum over the central range at RHIC and Tevatron energies is predicted.

The search for scaling violation of π^0 -meson formation in hadron-hadron, hadron-nucleus and nucleus-nucleus collisions, especially over a high transverse momentum range, could be very interesting for our understanding such fundamental problems as hadronization and phase transition of nuclear matter.

References

- [1] In: Proceedings Conference "Hard Processes in Hadronic Interactions", eds H.Satz and X.-N.Wang, Int. J. Mod. Phys. **A10**, 2881 (1995).
- [2] X.-N. Wang, Phys. Rev. **C58**, 2321 (1998).
- [3] X.-N. Wang, nucl-th/9812021; nucl-th/9907093.
- [4] R.P. Feynman, *Photon-Hadron Interaction* (Benjamin, New York, 1972).
- [5] I.Zborovsky, Yu.A.Panebratsev, M.V.Tokarev, G.P.Skoro, Phys. Rev. **D54**, 5548 (1996).
- [6] I.Zborovsky, M.V.Tokarev, Yu.A.Panebratsev, G.P.Škoro, Phys. Rev. **C59**, 2227 (1999).
- [7] M.V.Tokarev, I.Zborovsky, Yu.A.Panebratsev, G.P.Škoro, JINR Preprint E2-99-113, Dubna, 1999.
- [8] M.V.Tokarev, JINR Preprint E2-98-92, Dubna, 1998.
- [9] M.V.Tokarev, JINR Preprint E2-98-161, Dubna, 1998.
- [10] M.V.Tokarev, E.V.Potrebenikova, Computer Physics Communications **117**, 229 (1999).
- [11] M.V.Tokarev, T.G.Dedovich, JINR Preprint E2-99-300, Dubna, 1999.
- [12] L. Nottale, *Fractal Space-Time and Microphysics* (World Scientific, Singapore, 1992).
- [13] V.S. Stavinsky, Particles and Nuclei **10**, 949 (1979).
- [14] A.L.S.Angelis *et al.*, Phys. Lett. **B79**, 505 (1978).
- [15] C.Kourkouvelis *et al.*, Phys. Lett. **B83**, 257 (1979).
- [16] C.Kourkouvelis *et al.*, Phys. Lett. **B84**, 271 (1979).
- [17] C.Kourkouvelis *et al.*, Z.Phys. **5**, 95 (1980).
- [18] D.Lloyd Owen *et al.*, Phys. Rev. Lett. **45**, 89 (1980).
- [19] T.Akesson *et al.*, Z.Phys. **C18**, 5 (1983).
- [20] T.Akesson *et al.*, CERN-EP/89-98.
- [21] K.Eggert *et al.*, Nucl. Phys. **B98**, 49 (1975).
- [22] F.W.Busser *et al.*, Nucl. Phys. **B106**, 1 (1976).
- [23] P.Darriulat *et al.*, Nucl. Phys. **B110**, 365 (1976).
- [24] A.G.Clark *et al.*, Phys. Lett. **B74**, 267 (1978).
- [25] A.G.Clark *et al.*, Nucl. Phys. **B142**, 189 (1978).
- [26] M.Banner *et al.*, Phys. Lett. **115B**, 59 (1982).
- [27] W. Thomé *et al.*, Nucl. Phys. **B129**, 365 (1977).
- [28] D.R. Ward, Report No. CERN-EP/87-178, 1987 (unpublished).
- [29] F. Abe *et al.*, Phys. Rev. **D41**, 2330 (1990).
- [30] M. Adamus *et al.*, IHEP Preprint 88-121, Serpukhov, 1988.
- [31] G. Aler *et al.*, Z.Phys. **C33** (1986) 2330.
- [32] C.Kourkouvelis *et al.*, Phys. Lett. **B84**, 277 (1979).
- [33] J.D.Bjorken, Int.J.Mod.Phys. **A7** (1992) 4189;
J.D.Bjorken, K.L.Kowalski, C.C.Taylor, SLAC-PUB-6109, April, 1993.

Received by Publishing Department
on December 3, 1999.